Synthesis and Characterization of High-Density Polypropylene-Grafted Polyethylene via a Macromolecular Reaction and Its Rheological Behavior

Zhen Yao,[1] Zhan-Quan Lu,[1] Xi Zhao,[1] Bang-Wei Qu,[1] Zhi-Cheng Shen,[1] Kun Cao[1,2]

[1]*State Key Laboratory of Chemical Engineering, Institute of Polymerization and Polymer Engineering, Department of Chemical Engineering, Zhejiang University, Hangzhou 310027, China*
[2]*State Key Laboratory of Chemical Engineering, Unilab Research Center of Chemical Reaction Engineering, School of Chemical Engineering, East China University of Science and Technology, Shanghai 200237, China*

Received 25 January 2008; accepted 21 August 2008
DOI 10.1002/app.29229
Published online 25 November 2008 in Wiley InterScience (www.interscience.wiley.com).

ABSTRACT: High-density polyethylene grafted isotactic polypropylene (PP-*g*-HDPE) was prepared by the imidization reaction between maleic anhydride grafted polyethylene and amine-grafted polypropylene in a xylene solution. The branch density was adjusted by changes in the molar ratio between maleic anhydride and primary amine groups. Dynamic rheology tests were conducted to compare the rheological properties of linear polyolefins and long-chain-branched polyolefins. The effects of the density of long-chain branches on the rheological properties were also investigated. It was found that long-chain-branched hybrid polyolefins had a higher storage modulus at a low frequency, a higher zero shear viscosity, a reduced phase angle, enhanced shear sensitivities, and a longer relaxation time. As the branch density was increased, the characteristics of the long-chain-branched structure became profounder. The flow activation energy of PP-*g*-HDPE was lower than that of neat maleic anhydride grafted polypropylene (PP-*g*-MAH) because of the lower flow activation energy of maleic anhydride grafted high-density polyethylene (HDPE-*g*-MAH). However, the flow activation energy of PP-*g*-HDPE was higher than that of PP-*g*-MAH/HDPE-*g*-MAH blends because of the presence of long-chain branches. © 2008 Wiley Periodicals, Inc. J Appl Polym Sci 111: 2553–2561, 2009

Key words: branched; graft copolymers; polyolefins; rheology

INTRODUCTION

Isotactic polypropylene (iPP) is one of the most widely used polyolefins because of its outstanding physical and chemical properties, such as stiffness, excellent resistance to chemicals, a relatively high deformation temperature, and low density. However, the melt strength of commodity iPP drops rapidly as the temperature rises. The low melt strength of iPP leads to poor processing properties in extensional flow-dominated processes, such as thermoforming, extrusion coating, blow molding, and foaming. It is necessary to improve the melt strength of iPP to further widen its applications.

Grafting long-chain branches (LCBs) onto the iPP backbone is the most effective way to improve its melt strength. Various methods have been developed to produce long-chain-branched polypropylene (LCBPP). One method is in-reactor homopolymerization[1] and copolymerization.[2,3] Usually, macromonomers with terminal carbon–carbon double bonds are used as comonomers to produce branched polypropylene (PP) with a three-way-intersection topological structure. However, long-chain macromonomers are highly entangled; consequently, they have less mobility to diffuse toward the active centers. Therefore, the length of branch chains and the branch density (BD) are limited. The other method is a postreactor reaction, including electron-beam irradiation[4–10] and peroxide curing.[11–14] The branches are generated through radical-induced random chain scission followed by recombination. These processes are difficult to control, and the structures are complex. A new method for producing well-defined LCBPP involves the reaction between functionalized polymers. Lu et al.[15] prepared amine-functionalized PP by the reactive blending of maleic anhydride grafted polypropylene (PP-*g*-MAH) and diamines, and they obtained side-chain-extension PP. Lu and Chung[16] reported that LCBPP with a well-defined comb-like structure was synthesized through the reaction between PP-*g*-MAH and PP with an amine group at the end of the polymer chain (PP-*t*-NH_2). The

Correspondence to: K. Cao (kcao@che.zju.edu.cn).
Contract grant sponsor: National Natural Science Foundation of China (through Major Project 50390097 and Project 50773069).

structure of the obtained copolymer was controllable: BD could be controlled by the variation of the molar ratio of maleic anhydride (MAH) to the primary amine group, and the length of the branches could be tailored by the variation of the molecular weight of PP-*t*-NH_2.

Blending with a polymer with a distinctly higher melt strength than iPP, such as polyethylene (PE), is another previously widely used method to improve iPP's melt strength. Jahani and Barikani[17] blended iPP with ethylene–propylene–diene monomer, high-density polyethylene (HDPE), and LCBPP to increase the molecular entanglements and melt strength. The most significant effect was observed with PE and LCBPP used simultaneously. Physical blending is easy to perform, but it has its disadvantages. The poor compatibility of different polyolefins may cause phase separation in blends and lead to poor mechanical properties. To solve this problem, Graebling et al.[18] added a suitable peroxide initiator when blending PP and PE in an extruder. The product showed distinct strain hardening in elongational flow. Braun et al.[19] studied chain degradation, crosslinking, and grafting of PP and PE blends initiated by a peroxide reagent in the solution and melt, and they found that grafting reactions occurred only in the blend solutions and that the two polymers reacted fairly independently of each other in the blend melts; PP was degraded and PE was crosslinked because of the immiscible blends. It is very difficult to confirm the structures of products clearly. The synthesis of polyolefin-grafted copolymers by reactive extrusion or other forms of melt-phase processing was systemically reviewed by Moad,[20] and interchain functional polymer reactions to form graft copolymers have been addressed.

Most recently, Kashiwa et al.[21] prepared PE-*g*-PP and PP-grafted ethylene–propylene rubber by adopting a coupling reaction between terminally hydroxylated polyolefins (terminally hydroxylated PP) and MAH-grafted polyolefins [maleic anhydride grafted polyethylene (PE-*g*-MAH) or MAH-grafted ethylene–propylene rubber]. Similar work[22] has been found for the synthesis of PE-*b*-PP and PE-*g*-PP copolymers. The aforementioned study focused on morphology changes. However, the correlative structure and rheological properties of the final products were not involved.

This study was designed to graft HDPE chains onto a PP backbone with a confirmable structure via the reaction between the functional groups. Reactions between maleic anhydride grafted high-density polyethylene (HDPE-*g*-MAH) and amine-grafted polypropylene (PP-*g*-NH_2) were carried out to obtain high-density polyethylene grafted polypropylene (PP-*g*-HDPE). The rheological behavior of the resultant PP-*g*-HDPEs with different BDs was studied and compared with that of the starting polyolefins and their blends.

EXPERIMENTAL

Materials and preparation

PP-*g*-MAH was prepared in our laboratory by reactive extrusion in the presence of supercritical carbon dioxide with a process similar to that in the published literature[23] [weight-average molecular weight (M_w) = 139 kg/mol, number-average molecular weight (M_n) = 50 kg/mol, grafting degree = 0.51%]. HDPE-*g*-MAH was purchased from Dalian Haizhou Co. (Dilian, China; M_w = 80 kg/mol, M_n = 11.5 kg/mol, grafting degree = 0.19%). To purify the materials, PP-*g*-MAH and HDPE-*g*-MAH were dissolved separately in xylene at 130°C, precipitated in acetone, and dried at 70°C under vacuum conditions for 18 h to remove the residual MAH. Ethylenediamine (EDA), xylene, acetone, and ethanol were acquired from Hangzhou Changqing Chemical Reagent Co., Ltd. (Hangzhou, China).

Synthesis of PP-*g*-HDPE

PP-*g*-HDPE was synthesized through the reaction between HDPE-*g*-MAH and PP-*g*-NH_2. The reaction processes included two steps:

1. PP-*g*-MAH was reacted with a 10-fold excess of EDA at 130°C for 6 h in a xylene solution. After the imidization reaction, the product was precipitated in acetone and then was washed with ethanol and dried at 80°C *in vacuo* for 18 h to remove residual EDA.
2. The graft reaction was carried out by intensive mixing of HDPE-*g*-MAH and PP-*g*-NH_2 in a xylene solution at 130°C for 6 h. The final product was precipitated in acetone, washed with ethanol, and dried at 80°C *in vacuo* for 18 h.

The reactions involved in these two steps are shown in Figure 1, and the topological structures of the raw materials and obtained polymers are listed in Table I.

A PP-*g*-MAH/HDPE-*g*-MAH blend was prepared with the aforementioned PP-*g*-MAH and HDPE-*g*-MAH in a xylene solution. To make sure that the two polyolefins mixed well with each other, the polymer/solution mixture was stirred for 0.5 h after raw polyolefins were dissolved in solution. For comparison with the grafting copolymer, the PP and HDPE contents in the PP-*g*-MAH and HDPE-*g*-MAH blends were the same with PP-*g*-HDPE (R = 1, where R is the molar ratio of MAH to NH_2).

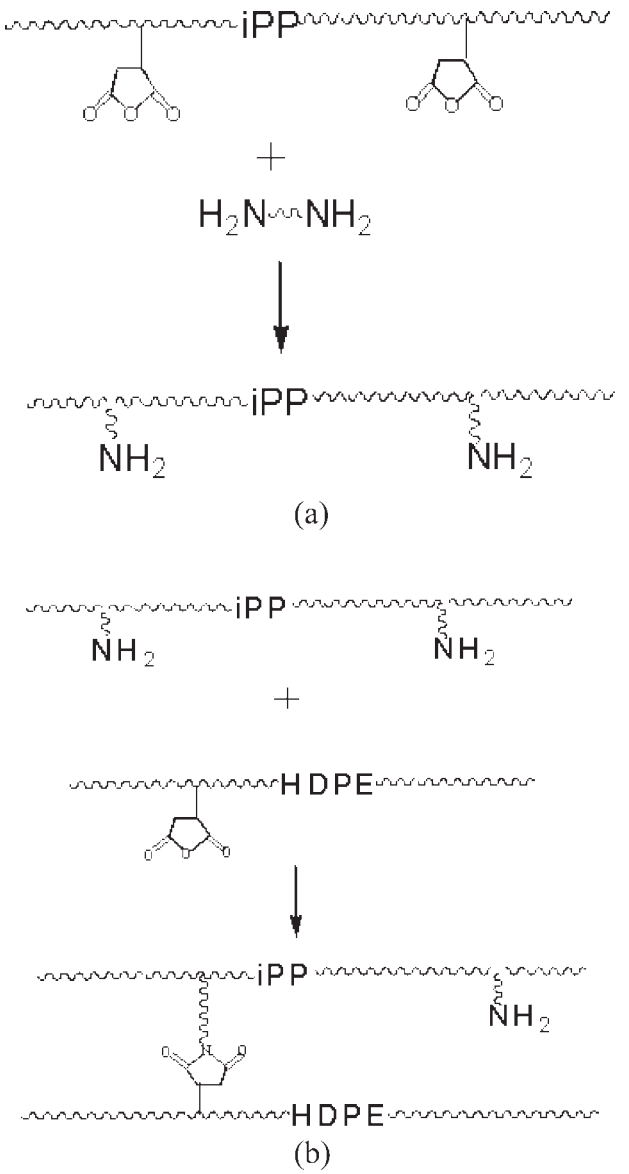

Figure 1 (a) Preparation of PP-*g*-NH_2 by the reaction of PP-*g*-MAH with 10-fold EDA in the solvent xylene at 130°C for 6 h. (b) Preparation of PP-*g*-HDPE by the reaction of HDPE-*g*-MAH with PP-*g*-NH_2 at 130°C for 6 h.

Characterization

Composition

The compositions of the raw polyolefins and obtained polymers were measured by Fourier transform infrared (FTIR). Samples for FTIR measurement were pressed into 8-μm-thick films under the conditions of 180°C and 100 kgf/cm^2. FTIR was carried out under a dry nitrogen atmosphere with a Nicolet 5700 IR spectrometer (Madison, Wisconsin) with Omnic software for data collection and analysis.

Intrinsic viscosity

The intrinsic viscosities of the raw polyolefins and obtained polymers were measured with an Ostwald viscometer (Hangzhou Shengli Chemical Co. Ltd., Hangzhou, China) at 135°C with decahydronaphthalene as the solvent.

Molecular weight

The molecular weights of the raw polyolefins and obtained polymers were measured with high-temperature gel permeation chromatography (GPC; PL-220, Polymer Laboratories). The polymer samples were dissolved in 1,2,4-trichlorobenzene (Essex Road/England) at a concentration of 0.1 mg/mL and measured at 150°C with a flow rate of 1 mL/min.

Rheology

The rheological behavior was measured on an ARES apparatus (TA, Rheometrics) [Castle, Delaware] with parallel plates with a diameter of 250 mm and a gap of 1.5 mm. Cylindrical samples of a thickness of 2 mm and a diameter of 25 mm were prepared by compression molding at 180°C. The different dynamic rheology tests and conditions are summarized as follows.

Dynamic time sweep measurements were carried out at 180°C for 10 min, which was long enough to finish other rheology tests, and the shear strain and shear frequency were fixed at 1% and 0.1 rad/s, respectively.

Dynamic strain sweep measurements were carried out at a frequency of 0.1 rad/s at 180°C. The initial strain was 0.01%, and the final strain was 100.0%.

Dynamic frequency sweep measurements were carried out over an angular frequency (ω) range of 0.1 rad/s $< \omega <$ 100 rad/s at 170, 180, and 190°C. The shear strain was fixed at 1%.

Furthermore, melt flow index (MFR) data were obtained at 230°C with a melt flow indexer (Ceast) [Pianezza, Italy] with a load of 2.16 kg.

RESULTS AND DISCUSSION

Characterization of PP-*g*-HDPE by FTIR

As shown previously, HDPE was grafted onto PP through the reaction of functional groups, so FTIR is an effective way of detecting the reaction degree. Figure 2 compares the FTIR spectra of the starting polyolefins PP-*g*-MAH and HDPE-*g*-MAH, PP-*g*-NH_2 formed through the first reaction step, and PP-*g*-HDPE synthesized by the reaction of HDPE-*g*-MAH with PP-*g*-NH_2. The absorption band at 1783 cm^{-1} for PP-*g*-MAH (1790 cm^{-1} for HDPE-*g*-MAH), together with two shoulders at 1860 (weak) and 1725 cm^{-1} (1728 cm^{-1} for HDPE-*g*-MAH), was assigned to the carbonyl group (>C=O) of the cyclic anhydride, which almost disappeared when PP-*g*-MAH

TABLE I
Summarized Structures of the Starting and Obtained Polyolefins

Sample	Structure parameters	Topological structure
PP-*g*-MAH	MAH-grafted PP with an average of 2.6 MAH groups on each polymer chain and M_n = 50 kg/mol	
PP-*g*-NH_2	NH_2-grafted PP, a product of the reaction between PP-*g*-MAH and a 10-fold excess of EDA	
HDPE-*g*-MAH	MAH-grafted HDPE with an average of 0.2 MAH groups on each chain and M_n = 11.5 kg/mol	
PP-*g*-HDPE	PP-grafted HDPE with a 1.2-LCB structure and with *R* varying from 0.5 to 2	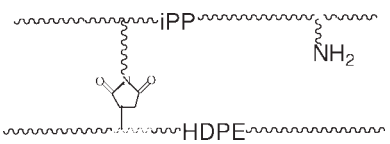

reacted with EDA or HDPE-*g*-MAH reacted with PP-*g*-NH_2. A new strong peak appeared at 1707 cm^{-1} for PP-*g*-NH_2 (1712 cm^{-1} for PP-*g*-HDPE), corresponding to the newly formed imide groups. All these results indicated a complete conversion of grafted MAH with NH_2 groups.

Molecular weight

After the grafting reaction, the molecular weight should increase. However, the Mark–Houwink constants of PP and HDPE are different, so it is hard to calculate the real molecular weight from the GPC curve. Figure 3 shows the GPC curves of the starting polyolefins HDPE-*g*-MAH and PP-*g*-MAH and the grafted product PP-*g*-HDPE. Compared with the two raw polyolefins, the product PP-*g*-HDPE showed a shorter elution time, which implied that the molecular weight of the product was increased after imidization.

Because the topological structures of raw polyolefins and obtained polymers are well defined and the graft reactions proceed to almost 100% conversion, as shown in FTIR spectra, we can roughly calculate BD, which is defined as the number-average LCB per 1000 carbons. In PP-*g*-MAH in Table I, there are on average 2.6 MAH groups on each polymer chain as calculated from its grafting degree and molecular weight. PP-*g*-NH_2 was formed by the reaction of PP-*g*-MAH with a 10-fold excess of EDA; therefore, PP-*g*-NH_2 also has 2.6 NH_2 groups on each polymer chain. However, there are on average 0.2 MAH groups on each HDPE-*g*-MAH chain (Table I). It is obvious that BD can be calculated with the following equation:

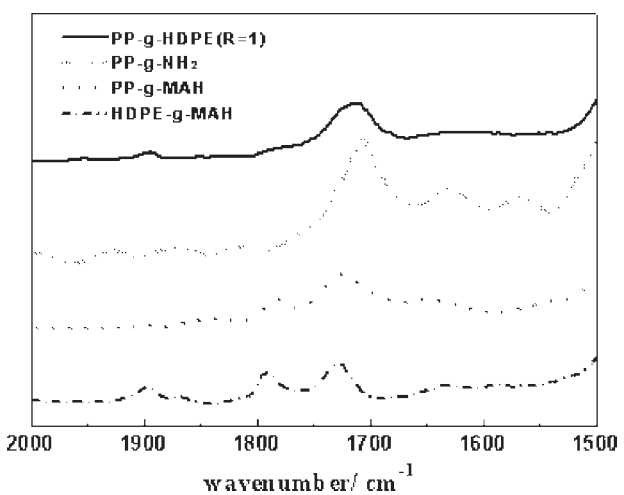

Figure 2 FTIR spectra of PP-*g*-MAH, HDPE-*g*-MAH, PP-*g*-NH_2, and PP-*g*-HDPE (R = 1).

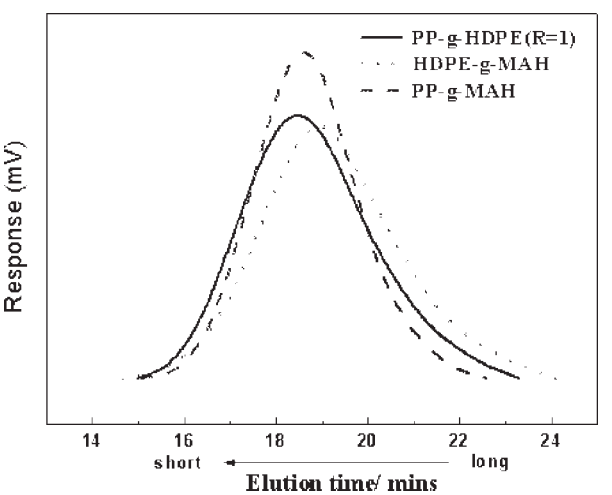

Figure 3 GPC curves of PP-*g*-MAH, HDPE-*g*-MAH, and PP-*g*-HDPE (R = 1).

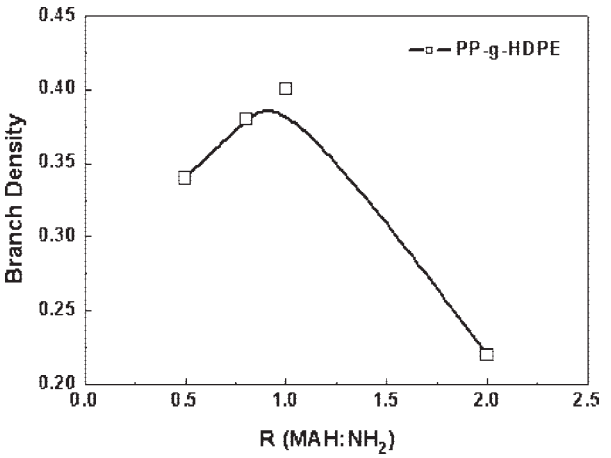

Figure 4 Effect of R on the average BD for the obtained polyolefins.

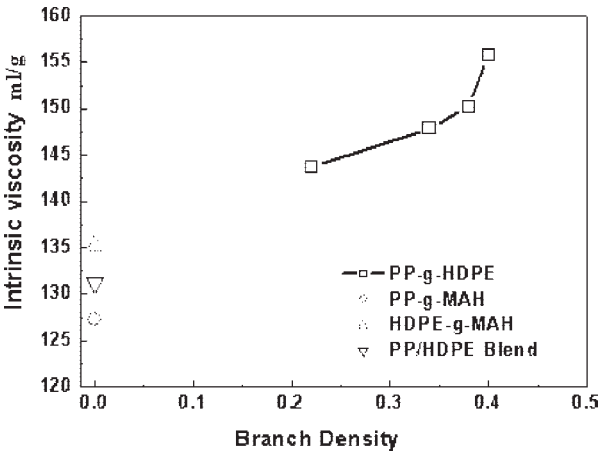

Figure 5 Intrintsic viscosity for PP-*g*-MAH, HDPE-*g*-MAH, PP-*g*-MAH/HDPE-*g*-MAH blends, and PP-*g*-HDPE with different BDs.

$$\mathrm{BD}_{\mathrm{PP}-g-\mathrm{PE}} = \frac{2.6 \times K \times 2 \times 100}{\frac{Mn_{\mathrm{PP}-g-\mathrm{NH_2}} \times 2}{42} + R \times \frac{2.6}{0.2} \times \frac{Mn_{\mathrm{PE}-g-\mathrm{MAH}} \times 2}{28}}$$

$$\begin{cases} K = R, & \text{if } R \leq 1; \\ K = 1, & \text{if } R > 1; \end{cases}$$

where K is the degree of the reaction.

Figure 4 compares the BDs of the obtained polymers with different R values. In PP-*g*-HDPE, BD increased as R increased, and it reached a maximum value at $R = 1$. When R was greater than 1, HDPE-*g*-MAH was in excess, and BD decreased with increasing R. Because raw polyolefins PP-*g*-MAH and HDPE-*g*-MAH can be considered linear polymers, the BDs of these two samples and their blend are zero.

Figure 5 shows the intrinsic viscosity of the starting polyolefins and a series of resultant PP-*g*-HDPEs with different BDs. After the imidization, PP-*g*-HDPE expectably showed a much higher intrinsic viscosity than the raw polyolefins. As the BD increased, the intrinsic viscosity increased.

MFR

MFRs of the two starting polyolefins PP-*g*-MAH and HDPE-*g*-MAH and all the PP-*g*-HDPE products are listed in Table II. The MFRs of PP-*g*-MAH and HDPE-*g*-MAH were 29 and 9 g/10 min, respectively. However, MFRs of all PP-*g*-HDPEs were less than 0.1 g/10 min, and this meant that PP-*g*-HDPE could barely flow under these conditions. It was suspected that crosslinking took place during the reaction process. However, all PP-*g*-HDPEs were dissolved during the preparation process and intrinsic viscosity test. Furthermore, the average functionality of PP-*g*-MAH and HDPE-*g*-MAH was less than 2; it was impossible to gel in the designed graft reaction. Therefore, the dramatic reduction in the MFR of PP-*g*-HDPE cannot be contributed to crosslinking. One potential reason may be a magical effect of the given topological structure with a starlike cross. The PP-*g*-MAH/HDPE-*g*-MAH blend is also compared with PP-*g*-HDPE in Table II. Even though the two products had the same content of HDPE, the PP-*g*-MAH/HDPE-*g*-MAH blend had a much higher MFR than PP-*g*-HDPE ($R = 1$). It can be concluded that the change in the MFR was caused by the grafting of HDPE chains onto PP. To reveal how HDPE chains influence the rheological properties of PP, a dynamic rheology test was conducted.

Dynamic rheology test

To avoid possible complications caused by thermal degradation in the procedure of dynamic rheology tests, a thermal stability test was first carried out with a time sweep. As shown in Figure 6, the storage modulus (G') of PP-*g*-MAH changed from 2438 to 2153 Pa in 10 min (an 11.7% reduction). Maybe this was due to degradation during the test. It was

TABLE II
Melt Flow Rates of the Starting Polymer and Obtained Polymers

	PP-*g*-MAH	HDPE-*g*-MAH	PP-*g*-HDPE ($R = 0.5$)	PP-*g*-HDPE ($R = 0.8$)	PP-*g*-HDPE ($R = 1$)	PP-*g*-HDPE ($R = 2$)	PP-*g*-MAH/HDPE-*g*-MAH blend[a]
MFR (g/10 min)	29	9	0.08	0.07	0.09	0.07	15

[a] The PP and HDPE contents of the PP-*g*-MAH/HDPE-*g*-MAH blends were the same as those of PP-*g*-HDPE ($R = 1$).

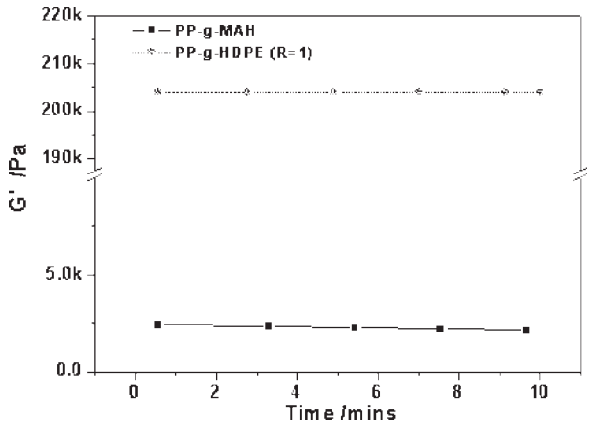

Figure 6 Determination of the thermal stability by the measurement of G' as a function of time at 180°C for PP-*g*-MAH.

unavoidable because we tried to minimize this effect by adding an antioxidant to the sample and using a nitrogen purge during the test. On the other hand, G' of PP-*g*-HDPE stayed at 204,000 Pa under the same test conditions. This can be explained as follows: PE is more stable in the melt than PP. Because most of the test samples contained PE-*g*-MAH, the degradation could be omitted, and the rheological properties were comparable.

To guarantee that the dynamic rheology tests would lie in the linear viscoelasticity zone, dynamic rheology measurements at different strains were taken. Figure 7 shows loss modulus (G'') curves plotted against the strain measured at 180°C for PP-*g*-MAH and PP-*g*-HDPE ($R = 1$). G'' of both samples remained at the same value as the strain was varied from 0 to 10%, and this belongs to the linear viscoelasticity zone. According to the aforementioned test results, the strain of all dynamic frequency sweep tests was fixed at 1% to make sure that the dynamic rheology test was located in the linear viscoelasticity zone.

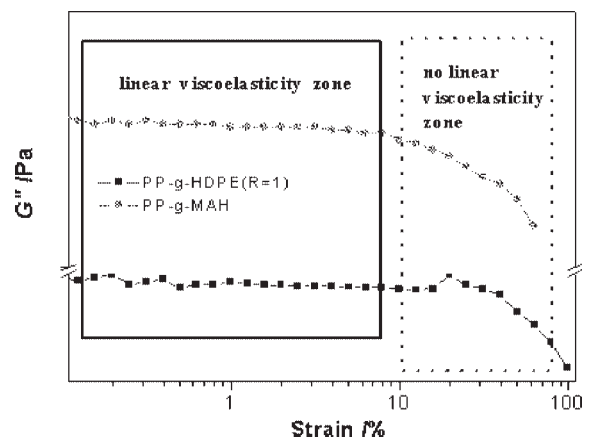

Figure 7 Determination of the linear viscoelasticity zone by the measurement of G'' as a function of strain at 180°C for PP-*g*-MAH.

Figure 8 shows G' as a function of the shear frequency for different samples. G' of PP-*g*-HDPE at low frequencies was much higher than that of the raw polyolefins. The change in G' that resulted from different BDs of PP-*g*-HDPE is also demonstrated in Figure 8. It can be seen that PP-*g*-HDPE with the highest BD has the highest value of G' at low frequencies. G' and G'' are both plotted versus the shear frequency in Figure 9. It is very interesting that no crossover between G' and G'' was found in most of the PP-*g*-HDPE samples; this is quite different from previously reported results.[24] A potential reason may be HDPE-*g*-MAH with a branched structure. When HDPE grafts onto PP, a hyperbranched structure is formed, and the rheological properties change.[25]

The curve of the loss angle (tan δ) as a function of the shear frequency has been used as a method of detecting the presence of LCBs.[26] DeMaio and Dong[27] reported that the melt strength is related to tan δ, suggesting that higher elasticity can lead to a higher melt strength. Gotsis et al.[28] also reported that the enhancement of the melt strength is related to the increase in the average number of LCBs per macromolecule. Consequently, increasing BD can lead to higher melt strength, higher elasticity, and lower tan δ. Figure 10 shows the tan δ plots of PP-*g*-MAH, HDPE-*g*-MAH, and PP-*g*-HDPEs with different BDs. It can be seen that PP-*g*-HDPE has a much lower tan δ value than the raw polyolefins, and this indicates the presence of LCBs in PP-*g*-HDPEs. With the increase in BD, tan δ of PP-*g*-HDPEs at low frequencies is decreased. As mentioned previously, an LCB structure usually shows a crossover of G' and G'' curves at which G' equals G'', and tan δ, defined as G''/G', is equal to 1 at the crossover. Because of the intensive reduction in the tan δ values of most obtained PP-*g*-HDPEs, the value of tan δ should always be below 1. Therefore, the crossover of G'

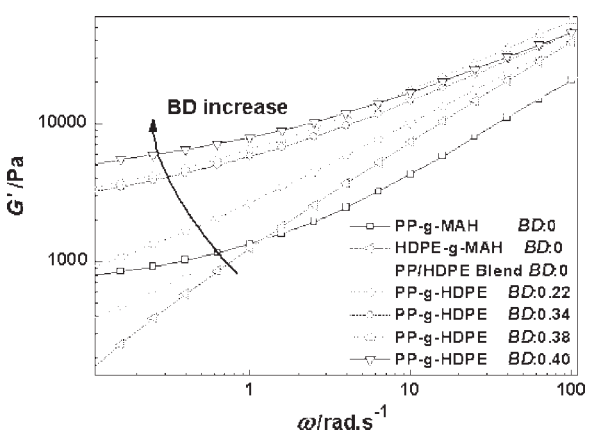

Figure 8 G' curves plotted against ω measured at 180°C for different samples.

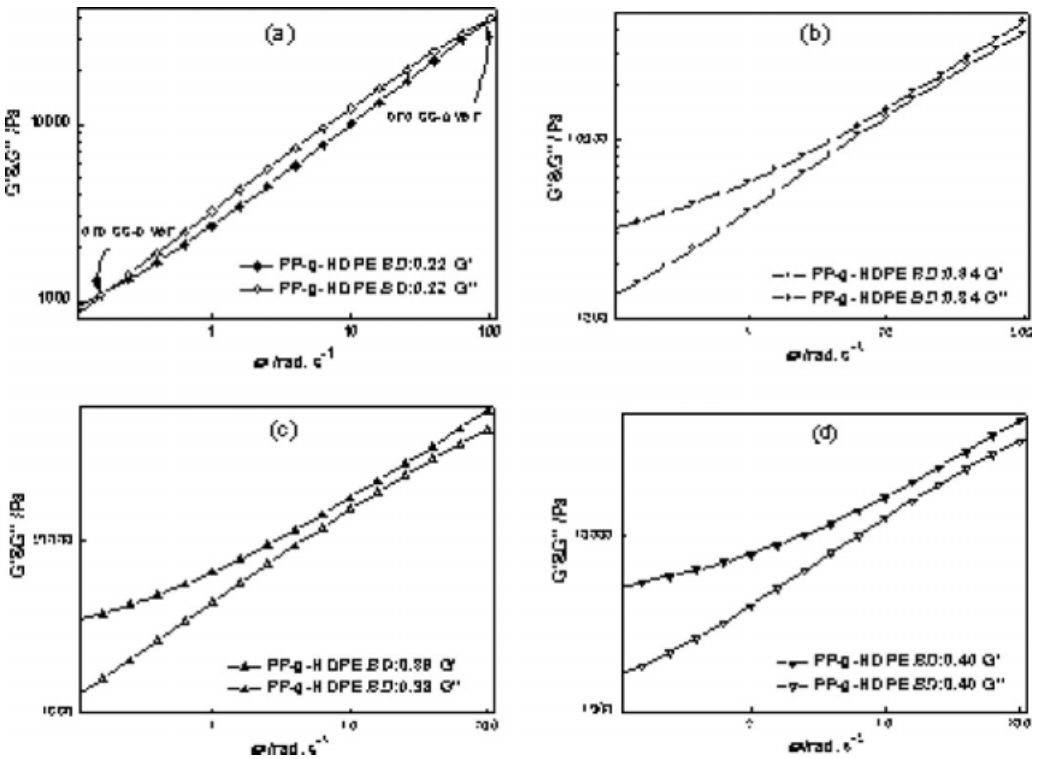

Figure 9 G' and G'' curves plotted against ω measured at 180°C for PP-*g*-HDPE with different BDs.

and G'' curves cannot be found. Nachbaur et al.[29] reported that a real material has viscoelastic behavior and that G' and G'' are finite. The material can exhibit solid-like behavior, with $G' \gg G''$, or liquid-like behavior, with $G' \ll G''$ in a low frequency range. Because tan δ is equal to G''/G', the sample exhibits solid-like behavior at tan $\delta < 1$, and the sample exhibits liquid-like behavior at tan $\delta > 1$. According to the tan δ curves plotted against the frequency in Figure 10, almost all samples except for HDPE-*g*-MAH and the PP/HDPE blend showed tan $\delta < 1$ in the low frequency region, and this means that solid-like behavior was found in these samples. The same conclusion can be reached from G' curves plotted against the frequency in Figure 8. Tan δ and G' are parameters of the melt elasticity, so the high elasticity of most of the samples led to their solid-like behavior.

The complex dynamic shear viscosity (η*) was measured over a range of ω values from 0.1 to 100 rad/s at 180°C. As shown in Figure 11, η* at a low frequency increased with an increase in BD.

Shear-thinning behavior is one of the pronounced characteristics of an LCB structure.[4,30] The relative

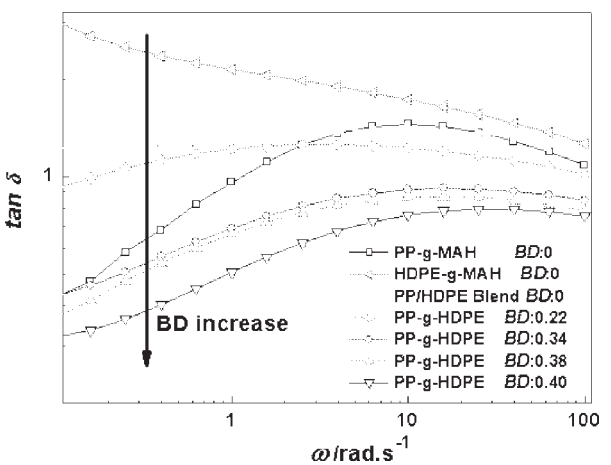

Figure 10 Tan δ curves plotted against ω at 180°C for PP-*g*-HDPE with different BDs.

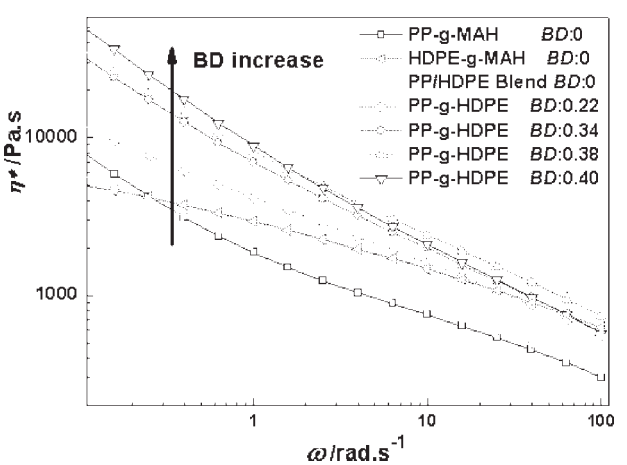

Figure 11 η* curves plotted against ω measured at 180°C for PP-*g*-HDPE with different BDs.

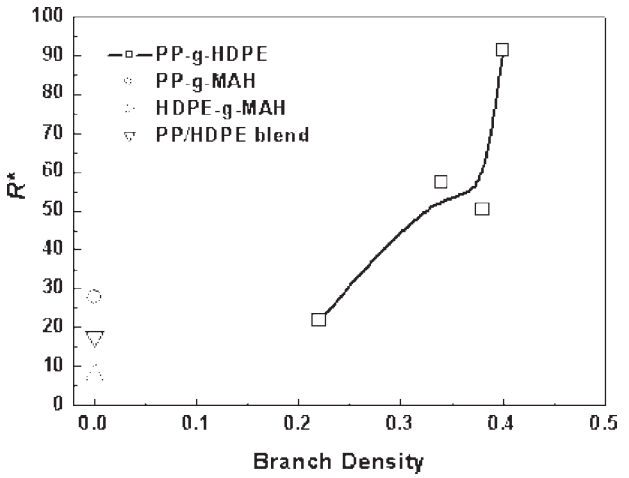

Figure 12 Determination of the shear sensitivities of the starting and obtained polymers at 180°C.

shear sensitivities can be expressed as the ratio of η* at different ω values. In this article, the ratio is denoted *R** and be calculated as follows:

$$R^* = \eta^*(0.1\text{rad/s})/\eta^*(100\text{rad/s})$$

Figure 12 compares the shear-thinning behavior of raw polyolefins PP-*g*-MAH and HDPE-*g*-MAH and resulting PP-*g*-HDPEs with various BDs. It can be seen that the higher BD is, the larger the value of *R** is.

Tsenoglou and Gotsis[31] reported that the zero-shear-frequency viscosity (η_0) of the LCB structure was increased with an increase in the degree of branching. η_0 can be calculated with the following equation:

$$\eta_0 = \lim_{\omega\to\infty} \eta' = \lim_{\omega\to\infty}\left[\frac{G''(\omega)}{\omega}\right]$$

Figure 13 shows η_0 values of PP-*g*-HDPEs with different BDs. Apparently, higher BD values led to increased η_0 values of PP-*g*-HDPEs.

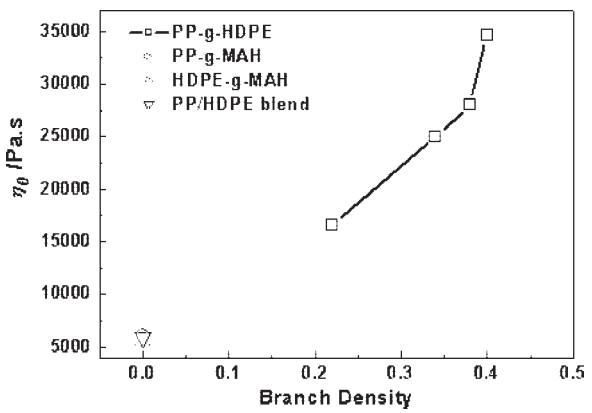

Figure 13 η_0 for the starting and obtained polymers at 180°C.

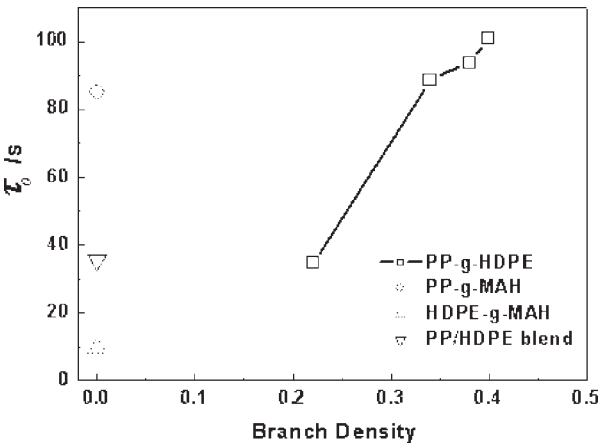

Figure 14 τ_0 for the starting and obtained polymers at 180°C.

A long relaxation time (τ_0) is an indication of the presence of an LCB structure. τ_0 can be calculated with the following equation:

$$\tau_0 = J_e^0 \times \eta_0$$

where J_e^0 is the steady-state compliance. It can be defined as follows:

$$J_e^0 = \frac{1}{\eta_0^2}\lim_{\omega\to\infty}\left[\frac{G'(\omega)}{\omega^2}\right]$$

Figure 14 shows τ_0 values of different PP-*g*-HDPEs. τ_0 increases with an increase in BD.

The flow activation energy (E_a) is used to evaluate the sensitivity of the rheological behavior to temperature. It has been found that LCB polymers have higher E_a values than linear polymers.[26] E_a is obtained by the application of the exponential relation accounting for the temperature dependence of the viscosity at temperatures far above the T_g or melting point. In this work, we chose two different temperatures, 170 and 190°C, and used the following equations to calculate E_a:

$$\eta_0(T) = A\exp(E_a/RT)$$

$$a_T(T) = \eta_0(T)/\eta_0(T_0)$$

$$a_T = \exp\left[\frac{E_a}{R}\left(\frac{1}{T}-\frac{1}{T_0}\right)\right]$$

$$E_a = \ln a_T \times R/\left(\frac{1}{T}-\frac{1}{T_0}\right)$$

where the a_T is the shift factor, the A is the pre-exponential factor, the T and T_0 are the Kelvin temperature. E_a values for different polyolefins are shown in Figure 15. PP-*g*-MAH has a higher E_a value than

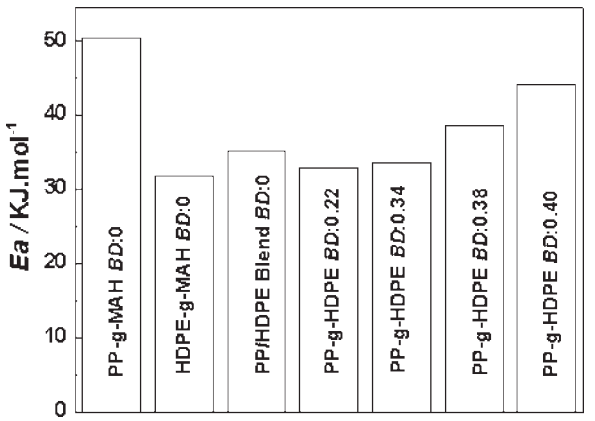

Figure 15 E_a for the starting and obtained polymers.

HDPE-*g*-MAH, and this indicates that the rheological behavior of PP-*g*-MAH is more sensitive to temperature than HDPE-*g*-MAH. Because of the presence of HDPE, all PP-*g*-HDPEs have lower E_a values than PP-*g*-MAH; this is quite different from normal LCBPP. The difference between PP-*g*-HDPE and PP-*g*-MAH/HDPE-*g*-MAH blends is also demonstrated in Figure 15. After the grafting of LCB, E_a becomes higher, and the higher BD is, the higher E_a of PP-*g*-HDPEs will be.

CONCLUSIONS

Long PE chains were grafted onto linear PPs to form PP-*g*-HDPEs by the reaction between PP-*g*-NH_2 and HDPE-*g*-MAH in a xylene solution. FTIR testing confirmed that the grafting reaction proceeded to almost 100% conversion. The BD was manipulated by the variation of *R*.

The creation of a starlike LCB structure showed a significant influence on the rheological properties of PP. As the BD was increased, G' at low frequencies was increased. However, crossover between G' and G'' was not found because tan δ was reduced and always less than 1. Higher shear sensitivity, η_0, and τ_0 values were found with an increase in the BD. The rheological behavior of PP-*g*-HDPE is less sensitive to temperature than that of PP-*g*-MAH because E_a of HDPE-*g*-MAH is lower than E_a of PP-*g*-MAH. However, E_a of PP-*g*-HDPE is higher than E_a of PP-*g*-MAH/HDPE-*g*-MAH blends because of the presence of the LCB structure.

The authors are indebted to Guo-Hua Hu (France) for helpful discussions.

References

1. Weng, W.; Hu, W.; Dekmezian, A. H.; Ruff, C. J. Macromolecules 2002, 35, 3838.
2. Kolodka, E.; Wang, W. J.; Zhu, S.; Hamielec, A. E. Macromolecules 2002, 35, 10062.
3. Ye, Z.; Alobaidi, F.; Zhu, S. Ind Eng Chem Res 2004, 43, 2860.
4. Auhl, D.; Stange, J.; Munstedt, H. Macromolecules 2004, 37, 9465.
5. Scheve, B. J.; Mayfield, J. W.; DeNicola, J.; Anthony, J. U.S. Pat. 5,731,362 (1998).
6. Yushii, F.; Makuuchi, K.; Kikukawa, S.; Tanaka, T.; Saitoh, J.; Koyama, K. J Appl Polym Sci 1996, 60, 617.
7. Saito, J.; Kikukawa, S.; Makuuchi, K.; Yoshii, F. U.S. Pat. 5,560,886 (1996).
8. Sugimoto, M.; Tanaka, T.; Masubuchi, Y.; Takimoto, J.; Koyama, K. J Appl Polym Sci 1999, 73, 1493.
9. Gao, J.; Lu, Y.; Wei, G.; Zhang, X.; Liu, Y.; Qiao, J. J Appl Polym Sci 2002, 85, 1758.
10. Lugao, A. B.; Cardoso, E. C. L.; Lima, L. F. C. P.; Hustzler, B.; Tokumoto, S. Nucl Instrum Methods Phys Res Sect B 2003, 208, 252.
11. Lagendijk, R. P.; Hogt, A. H.; Buijtenhuijs, A.; Gotsis, A. D. Polymer 2001, 42, 10035.
12. Wang, X.; Tzoganakis, C.; Rempel, G. L. J Appl Polym Sci 1996, 61, 1395.
13. Yu, Q.; Zhu, S. Polymer 1999, 40, 2961.
14. Graebling, D. Macromolecules 2002, 35, 4602.
15. Lu, Q. W.; Macosko, C. W.; Horrion, J. J Polym Sci Part A: Polym Chem 2005, 43, 4217.
16. Lu, B.; Chung, T. C. Macromolecules 1999, 32, 8678.
17. Jahani, Y.; Barikani, M. Iran Polym J 2005, 14, 693.
18. Graebling, D.; Lambla, M.; Wautier, H. J Appl Polym Sci 1997, 66, 809.
19. Braun, D.; Richter, S.; Hellmann, G. P.; Ratzsch, M. J Appl Polym Sci 1998, 68, 2019.
20. Moad, G. Prog Polym Sci 1999, 24, 81.
21. Kashiwa, N.; Kojoh, S.; Kawahara, N.; Matsuo, S.; Kaneko, H.; Matsugi, T. Macromol Symp 2003, 201, 319.
22. Vesely, T. Chem Listy 2005, 99, 486.
23. Dorscht, B. M.; Tzoganakis, C. Appl Polym Sci 2003, 87, 1116.
24. Gotsis, A. D.; Zeevenhoven, B. L. F.; Tsenoglou, C. Rheol J 2004, 48, 895.
25. Clarke, N.; De Luca, E.; Dodds, J. M.; Kimani, S. M.; Hutching, L. R. Eur Polym J 2008, 44, 665.
26. Wood-Adams, P. M.; Dealy, J. M.; Degroot, A. W.; Redwine, O. D. Macromolecules 2000, 33, 7489.
27. DeMaio, V.; Dong, D. Proc Soc Plast Eng Annu Tech Conf 1997, 43, 1512.
28. Gotsis, A. D.; Zeevenhoven, B. L. F.; Hogt, A. H. Polym Eng Sci 2004, 44, 1051.
29. Nachbaur, L.; Mutin, J. C.; Nonat, A.; Choplin, L. Cem Concr Res 2001, 31, 183.
30. Yan, D.; Wang, W. J.; Zhu, S. Polymer 1999, 40, 1737.
31. Tsenoglou, C. J.; Gotsis, A. D. Macromolecules 2001, 34, 4685.